Work function calculation of solid solution alloys using the image force model

Jonathan Avner Rothschild and Moshe Eizenberg*
Department of Materials Engineering, Technion, Israel Institute of Technology, Haifa 32000, Israel
(Received 31 December 2009; revised manuscript received 10 February 2010; published 3 June 2010)

The electronic work function of polycrystalline solid solution alloys is being analytically calculated using three different approaches. All approaches are derived by assuming that the alloys are in equilibrium and therefore surface segregation causes a difference between the surface composition and the bulk composition. An approach based on the image force, an approach based on the dipole layer formed due to electronegativity differences, and a simple surface concentration approach are compared to published experimental results. The image force model has a good agreement with the experiments, while the dipole-layer approach has a poor agreement, challenging the conventional concept of the double layer.

DOI: 10.1103/PhysRevB.81.224201 PACS number(s): 64.75.Nx, 73.30.+y

I. INTRODUCTION

The work function (WF) of alloys, along with other properties, is different from that of pure metals. Throughout the years, many techniques have been developed in order to calculate the WF of pure metallic surfaces. However, only few theoretical approaches for calculating the WF of alloys were introduced. A general model to calculate the WF as a function of composition would have many applications in the microelectronic industry as well as for catalysts.

The fundamental model for most calculations was based on the electrostatic potential of the lattice, which is determined by the charge distribution in the crystal.[1] The electrostatic potential becomes higher just outside the crystal and does not change further, this being defined as the free-electron level. The difference between the Fermi level (E_F) and the free-electron level is the first component of the work function. The dipole layer at the surface, which is also determined by the electron distribution, is the second component. The first self-consistent computation of the WF using the above-mentioned approach was done by Lang and Kohn[2] who used the jellium model. This model, which assumes a uniform background charge distribution in the crystal, included exchange and correlation effects, however, it was only accurate for the simple *s* metals. A more general approach was attempted by Skriver and Rosengaard[3] who used the Green's function technique. This approach was based on the linear muffin-tin orbitals (LMTO) with tight-binding and atomic-sphere approximations. For thin films, Fall *et al.*[4] used the local-density approximation (LDA) within the density-functional theory with the Ceperley-Alder exchange and correlation functional to measure the work function of Al.

A more phenomenological model was proposed by Brodie[5] and later modified by Halas and Durakiewicz.[6,7] In this model, the WF is calculated based on the electrostatic work that is needed in order to move an electron from a distance *d* above a conductive surface to infinity. The distance *d* was proposed to be the length of spontaneous polarization of the electron gas relative to the ionic lattice. The distance therefore depends on the electron-gas density *n* and the Fermi energy, relative to the ground state at the bottom of the electron band. Unlike sophisticated computational techniques, the predictions of this model fit well with experimental results for most polycrystalline metals. Furthermore, its simplicity makes it readily applicable for calculating the WF of metallic systems more complicated than pure elements.

The only analytical model for the WF of alloys was proposed by Gellat and Ehrenreich,[8] but it was only partial, referring strictly to the E_F shift and neglecting surface effects. Abrikosov and Skriver[9] used LMTO-coherent-potential approximation calculations to find the work function for three unsegregated alloys as a function of composition. The values calculated were about 1 eV higher than the experimental values. Leung *et al.*[10] studied the effect of an adsorbed monolayer of various elements on the WF of W using local-density-functional calculations within the framework of LDA. Their results confirm a linear correlation between the adsorbate-induced change in the surface dipole and the one in the WF. Their main conclusion was that the adsorbate-induced surface dipole does not depend only on the charge transfer and the electronegativity difference. Park *et al.*[11] used a similar method in order to calculate the WF of Al-Ni and Al-Pt systems. They showed the large impact of the surface atomic monolayer on the WF value, especially when the lower WF metal is on top. However, both binary systems exhibit very small mutual solubility and therefore the results cannot be verified by experiment.[12] Xu *et al.*[13,14] used a similar technique with the generalized gradient approximation and projector augmented wave pseudopotential for Ni-Pt and Mo-Ta binary systems. Since the solute atoms in all calculations were concentrated only in the surface atomic monolayer, a comparison with experiments might be difficult for these systems.

In this paper, three simple analytical models are proposed to calculate the WF variance of binary alloys as a function of composition. All three approaches deal with solid solution alloys at equilibrium, where the surface composition is different from the bulk composition. Theses models are extended to the cases of dual-phase compositions and amorphous alloys. The theoretical calculations are compared with published experimental data of binary systems which have large soluble regions.

II. ANALYTICAL APPROACHES

Due to a difference in the surface energy of different elements and the thermodynamic preference to lower the sur-

face energy, the equilibrium surface composition is different than the bulk composition. Since work function is a surface property, the analytical approaches should take the segregation phenomenon into account when calculating WF values of alloys in equilibrium. The calculation of WF for dual-phase compositions and for amorphous alloys is done differently than the calculation of solid solutions. These calculations are also explained below.

A. Image force approach

The formula which Halas and Durakiewicz derived according to the image force in order to calculate the WF of polycrystalline materials is[6]

$$\Phi = \frac{43.46\alpha}{r_s^{3/2}E_F^{1/2}}, \tag{1}$$

where α is an empirical parameter which is either unity for most metals or equals 0.86 for alkali metals, Ca, Sr, Ba, Ra, Tl, and rare-earth metals. For the latter, this is due to the lack of surface relaxation which decreases the electron densities at the surface. r_s is the density parameter which is the effective radius of the electronic volume and is related to the electronic density, n, by

$$r_s = 1.388n^{-1/3}, \tag{2}$$

where r_s is in atomic radius units, i.e., normalized by Bohr's radius (a_o0.529 Å) and n is in mole per cubic centimeter units. The electron density can be calculated by the atomic density and the valence z

$$n = \frac{z\rho}{M} = \frac{zN_{cell}}{V_{cell}N_A}, \tag{3}$$

where ρ is the density of the metal, M is the atomic mass, N_{cell} is the number of atoms in a unit cell, V_{cell} is the unit-cell volume, and N_A is Avogadro's constant.

Since in this approach the WF was calculated irrespective of surface structure and orientation, the results were compared with experimental WF values of polycrystalline metals. Values of single facets can be explained by stating that although the bulk parameters determine the work function, they could slightly vary near the surface. Therefore, higher surface concentration facets have greater surface electronic concentration and consequently have larger WF values.[15] For example,[16] in W, which has a base-centered-cubic unit cell, the highest work function is measured for the (110) plane while for Ir, which is fcc, the highest work function is for (111). For polycrystalline metals the effective WF value is an average between the WF of the different facets. However it is not straightforward to calculate the WF of a surface consisting of several different oriented grains.

In this work we postulate that a similar calculation can be made for solid solution alloys by determining the Fermi energy and the electronic concentration at the surface layer. For solution A-B, the electronic concentration can be calculated using Eq. (3), where z is determined according to the rule of mixture

$$z_{A\text{-}B} = x_A^s z_A + x_B^s z_B, \tag{4}$$

where x_i^s is the atomic fraction of element i at the surface. Assuming that the lattice parameter behaves according to Vegards law and that the lattice parameter does not change in the lateral direction, the cell volume of the surface layer is

$$V_{A\text{-}B} = (x_A^s a_A + x_B^s a_B)(x_A a_A + x_B a_B)^2, \tag{5}$$

where a is the lattice parameter and x_i is the atomic fraction of element i in the bulk. Incorporating Eqs. (4) and (5) into Eq. (2) yields

$$r_s = 1.388\left[\frac{N_A(x_A^s a_A + x_B^s a_B)(x_A a_A + x_B a_B)^2}{N_{cell}(x_A^s z_A + x_B^s z_B)}\right]^{1/3}. \tag{6}$$

The surface concentrations can be calculated using thermodynamic assumptions. For dilute ideal solutions, the most commonly known isotherm that relates bulk and surface concentrations of the solute is the Langmuir isotherm[17,18]

$$x_B^s = \frac{bx_B}{1 + bx_B}, \tag{7}$$

where b is the segregation coefficient. For undiluted solutions, the Mclean isotherm is more suitable[19,20]

$$x_B^s = \frac{bx_B}{1 - x_B + bx_B}. \tag{8}$$

For nonideal solutions there are more complicated expressions, where b depends on the intermixing energy and on the matrix structure. The general behavior though is similar even in nonideal solutions and an effective b can be extracted from experiments.

Calculations of the E_F using the simple free-electron gas model are only accurate for simple metals, since only the s-electron bands behave according to the model assumptions. The d-electron bands are more localized energetically. Therefore, a more complex numerical calculation is essential in order to determine the band structure, and only afterwards the occupancy can be derived. The high density of states (DOS) in d metals causes the E_F to be lower than expected by the free-electron gas model. Also, the effective DOS due to overlapping bands is accumulative.[21,22] The calculation of E_F with good agreement to experiments is possible using *ab initio* techniques which take into account the exchange potential of a many-body system.[23]

The E_F depends on both the crystallographic structure of the material and the element. For example, two materials with exactly the same structure which consist of two different elements would have two different E_F values. Therefore, the dependence of E_F on the composition of the solution is even more complicated. However, Gellat and Ehrenreich derived an analytical correlation between the E_F of a binary solution and its composition assuming that the E_F values of the pure constituents are known[8]

$$E_{F,A\text{-}B} = x_A E_{F,A} + x_B E_{F,B} + x_A x_B \left\{ \frac{(E_{F,A} - E_{F,B})[\mathrm{DOS}(E_F)_A - \mathrm{DOS}(E_F)_B]}{x_A \mathrm{DOS}(E_F)_A + x_B \mathrm{DOS}(E_F)_B} \right\}, \quad (9)$$

where $\mathrm{DOS}(E_F)$ is the total density of states of the pure constituent at the Fermi-energy level. This equation is based on the charge transfer between the two elements. In general, it means that E_F is biased toward the element with the higher $\mathrm{DOS}(E_F)$. The equation can also be written as[24]

$$E_{F,A\text{-}B} = x_A E_{F,A} + x_B E_{F,B} + x_A x_B \left[\frac{(E_{F,A} - E_{F,B})\left(\frac{\mathrm{DOS}(E_F)_A}{\mathrm{DOS}(E_F)_B} - 1 \right)}{x_A \frac{\mathrm{DOS}(E_F)_A}{\mathrm{DOS}(E_F)_B} + x_B} \right]. \quad (10)$$

The fraction $\frac{\mathrm{DOS}(E_F)_A}{\mathrm{DOS}(E_F)_B}$ is equal to the fraction $\frac{C_{e,A}}{C_{e,B}}$, where C_e is the electronic specific heat.[25]

Finally, the calculation of the WF is done by inserting Eqs. (6) and (10) into Eq. (1).

B. Dipole-layer approach

An alternative approach that we propose for calculating the WF of solid solutions is related to the charge transfer that occurs at the metal surface between the atoms in the surface layer and the atoms at the first layer beneath it. We assume that the atomic ratio at the layer beneath the surface is assumed to be approximately equal to the bulk atomic ratio.

The dipole-layer potential is calculated as the work needed to move an electron from one charged surface to an oppositely charged surface. The surface-charge density is σ_q and the distance between the surfaces is δ.

The work of the electron crossing these two layers is

$$D = \frac{q}{\varepsilon_0} \sigma_q \delta, \quad (11)$$

where ε_0 is the electron permittivity in vacuum and q is the electron charge. The surface-charge density is simply $\sigma_q = \sigma_d Q$, where σ_d is the surface-dipole density and Q is the charge of the dipole, which is calculated using Pauling's electronegativity values (χ) of the different elements. It is given by the ionic character of the bonding times the electron charge[26]

$$Q = q[1 - e^{-0.25(\chi_A - \chi_B)^2}]. \quad (12)$$

The net dipole density is determined by both the surface atomic ratio x^s and the bulk atomic ratio x of each element. The net effect of the A-B dipoles is the density of A-B dipoles subtracted by the density of B-A dipoles

$$x_{A\text{-}B} = x_A x_B^s - x_B x_A^s. \quad (13)$$

The dipole density is $\sigma_d = x_{A\text{-}B} \sigma_a$, where σ_a is the atomic surface concentration. Both δ and σ_a should be calculated directly from the crystallographic structure and the orientation of the surface. A more general treatment, which might have a better fit with polycrystalline alloys, is done by approximating the linear atomic density to be $1/\delta$

$$n_a = \left(\frac{1}{\delta} \right)^3 \Rightarrow \delta = \left(\frac{1}{n_a} \right)^{1/3}, \quad (14)$$

where n_a is the atomic density. Similarly the relation between volume density and surface atomic density is $\sigma_a = n_a^{2/3}$. Inserting σ_q and δ into Eq. (11) yields

$$D = \pm \frac{q^2}{\varepsilon_0} n_a^{1/3} (x_A x_B^s - x_B x_A^s)[1 - e^{-0.25(\chi_A - \chi_B)^2}]. \quad (15)$$

The sign of the dipole depends on the charge transfer between A and B, where in case A has the larger electronegativity the charge transfer is toward A, making the A-B dipole negative and lowering the work function. The actual dipole is, in fact, quite smaller in magnitude due to depolarization effects. This effect is described by Topping's equation[27]

$$D_{dep} = \frac{D}{1 + 9\alpha\sigma_d^{3/2}}, \quad (16)$$

where α is the polarizability of the segregated atom and can be estimated by the covalent radius of the segregated atom R as αR^3.

Assuming that this is the only contribution to the WF due to surface effects, the rest of the WF is calculated by a rule of mixture of the bulk composition, and the total WF is therefore

$$\Phi_{A\text{-}B} = x_A \Phi_A + x_B \Phi_B + D_{dep}. \quad (17)$$

C. Simple surface mixture approach

The third approach that we propose is to assume that the electrostatic potential which affects the work function is determined only by the surface layer. In this sort of analysis, the work function of the solid solution should behave according to the mixture rule of the surface composition

$$\Phi_{A\text{-}B} = x_A^s \Phi_A + x_B \Phi_B^s. \quad (18)$$

D. Dual-phase compositions

In the nonsoluble compositions of the phase diagram, the equilibrium state of the material is a mixture of two stable phases. Each distinct phase has a different surface potential as a result of a different work function. This configuration is completely analogous to a polycrystalline pure metal with different WF facets. The effective surface potential of the material will be composed of the surface potential of its constituents. The surface of such materials can be treated like parallel capacitors of two capacitors with different potentials. Assuming that the ratio of the area of the surface for phase α and β equals the volume ratio of each phase we expect

$$\Phi_{\alpha\text{-}\beta} = x_\alpha \Phi_\alpha + x_\beta \Phi_\beta. \quad (19)$$

When the vacuum WF is measured using photoemission, this might not be such a straightforward calculation. The

reason for this is that more electrons escape the facets with the lower WF and therefore shifting the average WF closer to the lower value.

E. Amorphous alloys

When using gas-phase or plasma-based deposition methods, some metals and alloys form without long-range ordering. Such materials exhibit behavior of a mixture of atoms rather than a solid solution behavior. Assuming that the free-electron gas model fits the amorphous phase, the only parameters which are needed to calculate are the effective valence, the molecular mass, and the density. The valence and molar mass is assumed to behave according to the rule of mixtures

$$M_{A\text{-}B} = x_A M_A + x_B M_B. \tag{20}$$

The volumetric mass density ρ is calculated by dividing the total mass over the total volume

$$\rho_{A\text{-}B} = \frac{x_A M_A + x_B M_B}{x_A(M_A/\rho_A) + x_B(M_B/\rho_B)}. \tag{21}$$

Incorporating Eqs. (4), (20), and (21) into Eq. (3) yields

$$n_{A\text{-}B} = \frac{x_A z_A + x_B z_B}{x_A(M_A/\rho_A) + x_B(M_B/\rho_B)}. \tag{22}$$

The main difference from solid solution alloys is that amorphous alloys are not in equilibrium and the segregation phenomenon does not appear and thus the surface composition equals the bulk composition.

F. Calculating the surface segregation factor

Theoretical calculations for the segregation factor b of ideal solutions can be done using[18]

$$b = \exp\left(\frac{\gamma_A - \gamma_B}{\sigma_a k_B T}\right), \tag{23}$$

where γ is the surface energy. The values for the surface energy for various metals were summarized by Skriver and Rosengaard.[3] Even though segregation is more complicated than implied by Eqs. (7), (8), and (23), they outline the general trend of the segregation. Segregation depends on the orientation of the surface. Therefore, the segregation of polycrystalline materials is the average segregation of all facets. The best option in order to calculate the WF is first calculate the segregation behavior of the system. In this paper, the segregation behavior was extracted from experimental works of the studied binary systems.

III. RESULTS

The possible contributions to WF of a solution coming from either one of the above-discussed mechanisms cannot be excluded, but the contributions and agreement with experimental data can be discussed for each method. In this section, we compare the calculated and experimental WF values of binary alloys. The focus of this work is the behavior of the WF as a function of composition and not the calculation of the pure element WF value. Therefore, the WFs of the pure elements are taken from the experiments. Difference in WFs of pure elements between different experiments and between theories is attributed to differences in sample preparation and measurement techniques. According to the image-force approach, this deviation originates from the electronic concentration at the surface, in the same manner that different crystallographic orientations yield different WFs, and so the electronic concentration was fixed to fit the WF of the pure metals.

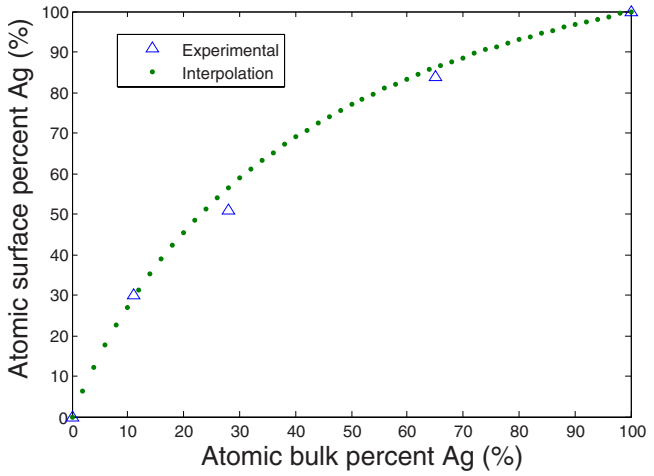

FIG. 1. (Color online) Ag surface concentration vs Ag bulk concentration. The triangles are the experimental points (Ref. 29). The open circles are the interpolation used in order to extract the effective segregation factor.

It is important to note that we compared between our theory and experiments only in systems where the vacuum WF was directly measured, since indirect measurements do not necessarily yield the vacuum WF values of the metals. For example, Schottky barrier heights can be determined by the metal/semiconductor interface just as much as by the metals WF.[28] Two different types of binary-alloy systems were used for the comparison. The Ag-Au and the Ag-Pd systems are without a miscibility gap while Cu-Ni and Au-Pt are with.

A. Alloy systems with full solubility: Ag-Au, Ag-Pd

The gold-silver system is known as a full solubility binary system which was studied both for its WF and its surface segregation.[29,30] The segregation behavior in this work is based on the experimental work done by Kelly *et al.* The experimental values are drawn in triangles in Fig. 1, showing the Ag surface concentration as a function of the Ag bulk concentration at a temperature of 500 °C.

The Mclean isotherm [Eq. (4)] was used in order to interpolate a surface-bulk concentration behavior which fits the experiment shown in the solid line in Fig. 1. The segregation factor was extracted to be approximately $b=0.3$.

The WF dependence on composition of the Ag-Au system was studied by Fain and McDavid.[30] The temperature during the deposition was 400–450 °C, indicating that the segregation behavior should be very similar to the one in Kelley's

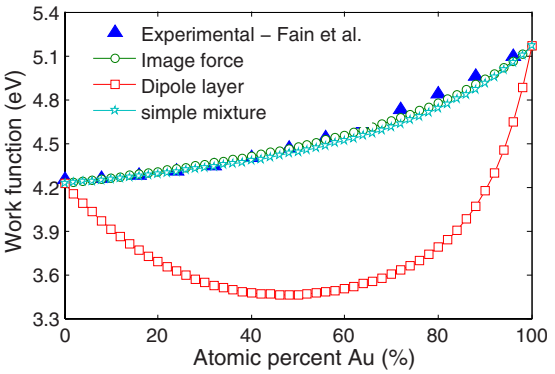

FIG. 2. (Color online) Work function variation with composition of the Ag-Au system.

experiments. The paper states that the work function was measured as a function of surface composition. However, the measurement was done by Auger electron spectroscopy (AES), which gives information which is deeper than the surface atomic layer. For the Au peak at 72 eV the mean free path is approximately 0.5 nm (Ref. 31) and the information depth is therefore about 1.5 nm (Ref. 32) under the surface. Therefore, the measured composition is the bulk composition of the alloys. Otherwise, the results would indicate that there is no surface segregation at all. The experimental results were interpolated by a quadratic function, which is marked by filled triangles in Fig. 2.

The image-force approach and the simple surface mixture approach yielded very similar results, which are in good agreement with the experimental results, showing a similar monotonic behavior. The dipole approach has a minimum near 50 at. % Au and deviates from the experimental results up to about 1.2 eV. This indicates that the dipole-layer approach has negligible effect in this system.

The silver-palladium system also exhibits full mutual solubility. The estimated segregation was made according to data from segregation experiments made at 323 °C.[33] The samples in the WF experiments were equilibrated at 300 °C and the surface concentration is therefore expected to be similar.[34] The results of the experimental measurements are plotted in Fig. 3.

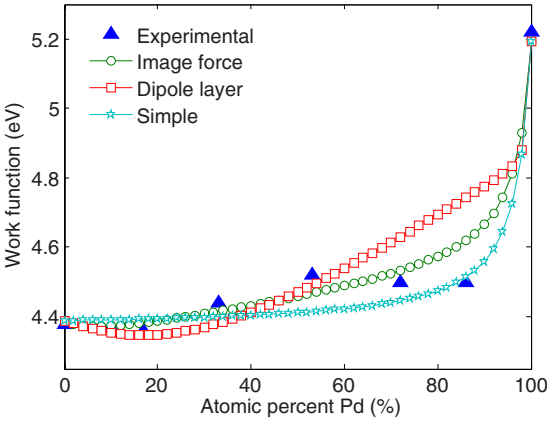

FIG. 3. (Color online) Work function variation with composition of the Ag-Pd system.

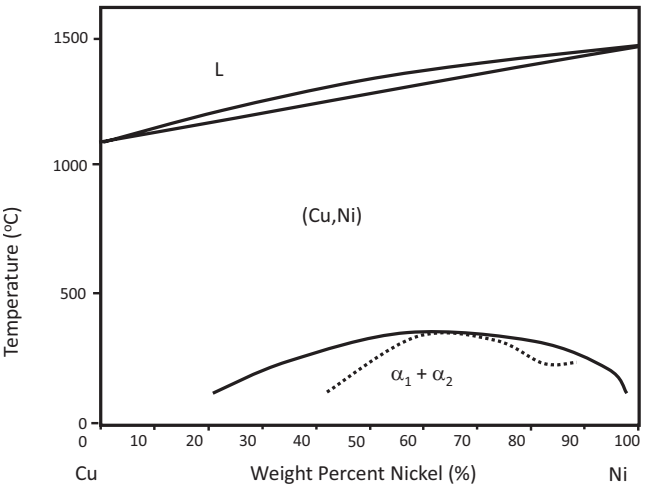

FIG. 4. Phase diagram of the Cu-Ni system (Ref. 12).

Much like the Ag-Au system, the experimental values are quite similar to the image force and simple surface mixture calculations. The dipole-layer model curve also has a good agreement to the experimental results. At some compositions, the dipole-layer model WF values are even closer to the experimental WF values than the other two models.

B. Alloy systems with a miscibility gap: Cu-Ni, Au-Pt

The copper-nickel binary system exhibits a phase-separation behavior beneath 400 °C, as shown in the phase diagram in Fig. 4. Several experimental works were done to measure the WF of copper-nickel alloys.[35–38] Sachtler and Dorgelo[35] measured the WF variation with the alloy composition after the Cu-Ni films were sintered and equilibrated at 200 °C. The compositions of the results, marked in filled triangles in shown in Fig. 5, were roughly estimated by x-ray diffraction measurements. The segregation behavior of this system at a temperature close to 200 °C was extracted from the results of several experimental and theoretical works.[9,39,40] The calculations were initially done overlooking the phase-separation phenomenon and the results are plotted

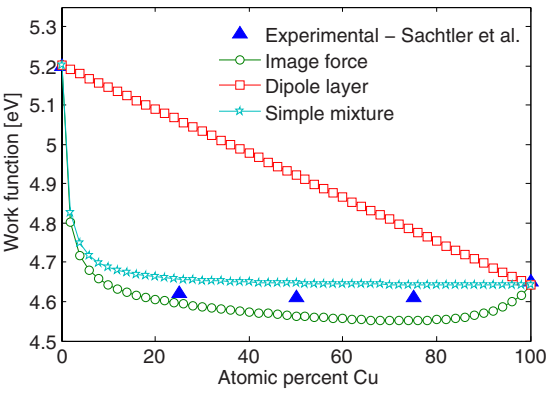

FIG. 5. (Color online) Work function variation with composition of the Cu-Ni system on sintered samples. In this system Cu atoms segregated to the surface.

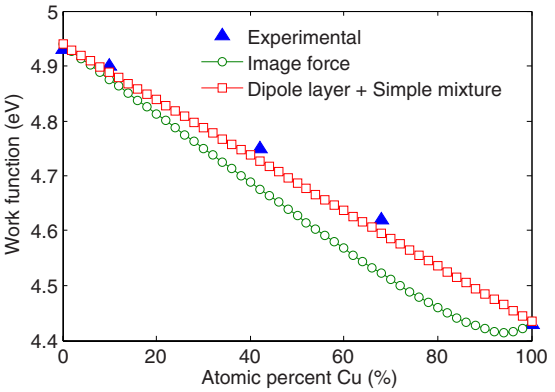

FIG. 6. (Color online) Work function variation with composition of the Cu-Ni system with presumably no segregation, due to sputtering of the surface layers.

in Fig. 5. The approach which has the closest results to the experiments is the simple surface rule of mixture. However, it cannot predict that the WF values of the alloy can be lower than the WF values of either pure metal. The image-force approach shows a large composition range with a WF value lower than the clean Cu. The dipole layer shows a linear behavior since the electronegativity of Cu is very close to that of Ni.

The next step in the WF calculations for the Cu-Ni system is taking into account the phase separation. This cannot be done simply using Eq. (19) since the surface composition of this system is constant independently from the bulk composition, as thermodynamically modeled and proved by hydrogen chemisorption experiments.[41,42] At 200 °C the alloy separates into a mixture of a Ni-rich phase with approximately 4 at. % Cu and a Cu-rich phase with approximately 70 at. % Cu. Using the segregation data at this temperature, the surface compositions of the Ni-rich phase and the Cu-rich phase should be 35 at. % Cu and 99 at. % Cu, respectively. The constant surface composition was determined to be 77 at. % Cu by the chemisorption experiments. Using the rule of mixture, the ratio between Ni-rich phase and the Cu-rich phase is approximately 3:7. Applying this ratio on Eq. (19) and taking the WF of the Ni-rich phase and the Cu-rich phase from Fig. 5, the calculated value of the WF is 4.65 eV, only 0.04 eV higher than the measured WF value and identical to the WF value measured for pure Cu. This can be attributed to the photoemission-based technique used, which is more sensitive to the WF of the Cu-rich phase which has a lower WF. Applying the same ratio between the Ni-rich phase and the Cu-rich phase for the simple surface mixture approach and the dipole-layer approach yields WF values of 4.7 eV and 4.92 eV, respectively.

In another experimental setup, the WF values of the Cu-Ni system without segregation were measured.[36] In order to achieve this, about one hundred layers were sputtered off from the surface of the samples in vacuum prior to the measurements. It should be noted that the sputtering process might have also caused the surface to become amorphous. The experimental results of the measured WF as a function of composition as measured by AES are plotted in Fig. 6 by filled triangles. Similar results were achieved by using the

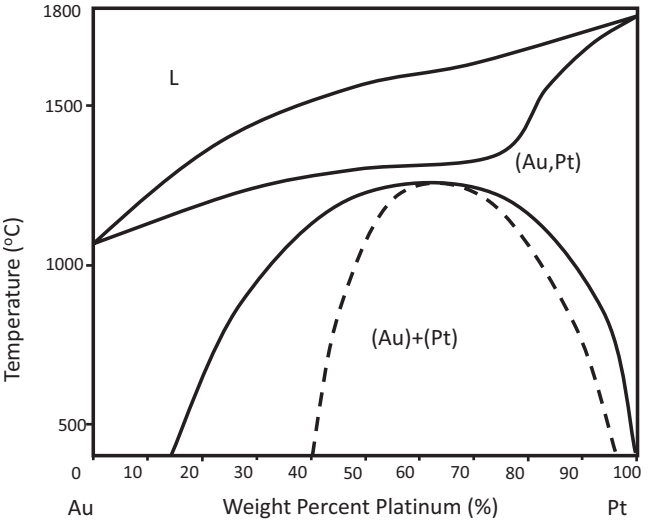

FIG. 7. Phase diagram of the Au-Pt system (Ref. 12).

field-emission method after cleaning the surface.[38] In this setup, no segregation is expected and therefore both the dipole-layer approach and the simple surface mixture give the same linear results. However, the image-force model shows a deviation from linearity, which is caused by the nonlinearity of the E_F variation with composition. Nevertheless, all models have a good agreement with the experimental results. Other experiments also approved the difference in WF between segregated samples and unsegregated samples in the Cu-Ni system.[37]

The miscibility gap in the gold-platinum binary system is quite large as seen in Fig. 7. However, the strong surface segregation is enough to cause a high Au content at the surface even at a composition very near pure Pt. Therefore, according to the dipole-layer approach, a negative dipole layer should be formed near the surface, increasing the work function. The two other approaches basically suggest that the surface Au should cause the work function values to be close to pure Au.

Bouwman and Sachtler[43] measured the WF variance with composition in the Au-Pt system after equilibrating the samples at 300 °C. Their results are plotted in filled triangles in Fig. 8. The WF value that they measured for Au was about 0.3 eV higher than known in literature for polycrystalline Au.

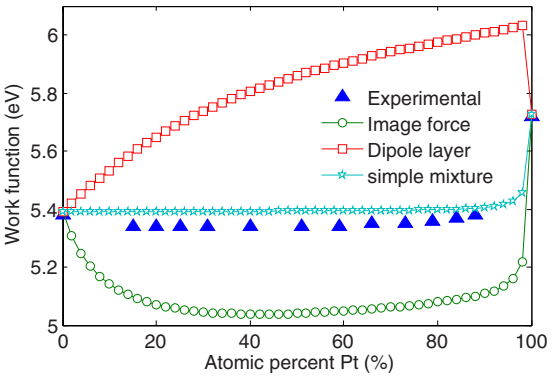

FIG. 8. (Color online) Work function variation with composition of the Au-Pt system.

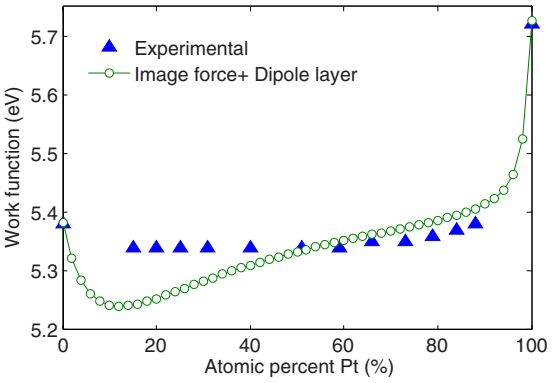

FIG. 9. (Color online) Work function variation with composition of the Au-Pt system.

This may indicate some preferred orientation with a higher work function. The WF value of nearly all compositions measured was slightly lower than the pure Au WF value. Similarly to the calculation for the Cu-Ni system, the results of the analytical models are plotted in Fig. 8 taking into account segregation but overlooking the phase separation.[9]

The minimum of the WF plot can only be explained by the image-force model, although the values predicted by the image-force model are lower by about 0.4 eV from the constant value of the alloy. On the other hand, the dipole-layer approach calculations show a behavior completely opposite to the experimental outcome. In fact, if the dipole layer exists it could be accounted for offsetting the effect of the image force. The accumulated effect of both models is plotted in Fig. 9.

At the temperature of 300 °C, the alloy is expected to separate into a Au-rich phase with a composition of approximately 12 at. % Pt and a Pt-rich phase with a composition of approximately 99.5 at. % Pt. The constant value of the alloy WF was believed to be attributed to a constant surface composition, due to a mechanism similar to the Cu-Ni system. Since no additional quantitative data were gathered on the surface composition of the alloy, it can be estimated by using the rule of mixture. Based on the image-force model, as plotted in Fig. 8, the ratio between the Au-rich phase and the Pt-rich phase is approximately 1:4. Based on the accumulated effect of, plotted in Fig. 9, the ratio between the Au-rich phase and the Pt-rich phase is approximately 7:3, which seems to be more reasonable.

IV. DISCUSSION

The fundamental result of this work is that segregation plays a major role in determining the WF of alloys. The reason for this is that the WF is a surface property and thus determined by the surface composition and structure. All three analytical models proposed were based on this assumption, which is clear from the experimental data of the Ag-Au, Cu-Ni, Au-Pt, and Ag-Pd systems. In all approaches, the experimental WF values of the pure metals should be known in order to allow accurate calculations of the WF variance with compositions. Also, the difference between the Cu-Ni system with segregation and without segregation is remarkable.

The simple surface mixture model seems to be close to the experimental results but cannot explain the minimum found in some systems. It is not very dissimilar even in those systems and therefore can yield fairly good approximation for the WF variance with composition even if only the WF values of the pure constituents are known, assuming that the surface atomic concentration is known.

The image-force approach, which is based mainly on the electron density at the surface, is in good agreement with experimental data to the extent of prediction of the minimum found beneath the pure metal WF values. The pure-metal WF values were used to fit the density of the electrons. A difference in surface electron density can be attributed to different surface structures, such as preferred orientation, defect concentration, and roughness, due to different sample preparation techniques.[44] Another reason to determine the electronic concentration according to the pure elements WF is that different techniques sometimes yield different results. For example, there is a 0.3 eV difference in the WF values of pure Ni measured for different experimental setups of the Cu-Ni system.[35,36] By fitting the electronic concentration, the theoretical calculations are not affected by variance due to preparation and measurement techniques. On the other hand, this means that the WF values are case determined according to the applied experimental setup.

The dipole layer due to the electronegativity difference model does not fit well with experiments. In some cases it even predicts a behavior which is contradictory to the experiment, such as in the Au-Pt binary system. On the other hand, it might be a complementary effect in this system. The Ag-Au system is the only system described in this work where the dipole-layer approach unquestionably fails. This is an important and even surprising point, since in surface science, the dipole of adsorbed adatoms on surfaces is considered to be the major cause for changes in the WF. Since there is no physical difference between adsorbed atoms and segregated atoms, similar dipole is expected. The poor agreement of experiments with these results, combined with the good agreement of experiments with the image-force approach results, call into question the entire double-layer concept. The double layer is used many times in surface science and in interface science to describe electronic phenomena. These phenomena might be explained by an alternative mechanism, perhaps by the image force and the change in electronic density at the material surface.

Both Cu-Ni and Au-Pt showed a behavior of constant surface compositions independent of the bulk composition in their respective miscibility gaps. In these systems, the surface composition is attributed first of all to the ratio between phases. The surface composition of each phase is a secondary effect, which is also invariant to the composition. Therefore the WF is constant inside the phase-separation region.

V. SUMMARY

There has been a lack in theoretical studies covering the WF of alloys, which is an important surface property. Computational models, which have been used in order to calculate the WF, can be used for this end, but their agreement

with even pure metals is not always good. Three analytical approaches to calculate the WF of solid solution alloys were presented. All of these approaches were based on the fact that the equilibrated surface composition of solid solution alloys is different from their bulk composition. The simple surface composition approach is the most trivial one and takes into account only the WF values of the pure constituents. The image force approach is more complicated and can predict WF values which are larger or smaller than the WF values of both pure metals. The dipole-layer approach yields the worst agreement with results and might rattle the conventional concept of the double layer.

ACKNOWLEDGMENTS

The authors would like to thank T. Maniv from the Chemistry department at the Technion for helpful discussions and the Russel Berrie Nanotechnology Institute (RBNI) for financial support.

*yonatanr@tx.technion.ac.il

[1] N. W. Ashcroft and D. N. Mermin, *Solid State Physics* (Thomson Learning, Toronto, 1976).
[2] N. D. Lang and W. Kohn, Phys. Rev. B **3**, 1215 (1971).
[3] H. L. Skriver and N. M. Rosengaard, Phys. Rev. B **46**, 7157 (1992).
[4] C. J. Fall, N. Binggeli, and A. Baldereschi, J. Phys.: Condens. Matter **11**, 2689 (1999).
[5] I. Brodie, Phys. Rev. B **51**, 13660 (1995).
[6] S. Halas and T. Durakiewicz, J. Phys.: Condens. Matter **10**, 10815 (1998).
[7] T. Durakiewicz, S. Halas, A. Arko, J. J. Joyce, and D. P. Moore, Phys. Rev. B **64**, 045101 (2001).
[8] C. D. Gelatt and H. Ehrenreich, Phys. Rev. B **10**, 398 (1974).
[9] I. A. Abrikosov and H. L. Skriver, Phys. Rev. B **47**, 16532 (1993).
[10] T. C. Leung, C. L. Kao, W. S. Su, Y. J. Feng, and C. T. Chan, Phys. Rev. B **68**, 195408 (2003).
[11] S. Park, L. Colombo, Y. Nishi, and K. Cho, Appl. Phys. Lett. **86**, 073118 (2005).
[12] *Binary Alloy Phase Diagrams*, edited by T. B. Massalski (American Society for Metals, Metals Park, Ohio, 1987).
[13] G. Xu, Q. Wu, Z. Chen, Z. Huang, R. Wu, and Y. P. Feng, Phys. Rev. B **78**, 115420 (2008).
[14] G. Xu, Q. Wu, Z. Chen, Z. Huang, and Y. P. Feng, J. Appl. Phys. **106**, 043708 (2009).
[15] K. Wojciechowski, Europhys. Lett. **38**, 135 (1997).
[16] H. B. Michaelson, J. Appl. Phys. **48**, 4729 (1977).
[17] J. J. Burton and E. S. Machlin, Phys. Rev. Lett. **37**, 1433 (1976).
[18] *Interfacial Segregation*, edited by W. C. Johnson and J. M. Blakely (American Society for Metals, Metals Park, Ohio, USA, 1979).
[19] P. A. Dowben and A. Miller, *Surface Segregation Phenomena* (CRC Press, Boca Raton, Florida, USA, 1990).
[20] M. P. Seah, J. Vac. Sci. Technol. **17**, 16 (1980).
[21] N. F. Mott and H. Jones, *The Theory of the Properties of Metals and Alloys* (Dover, New York, NY, 1958).
[22] A. H. Wilson, *The Theory of Metals*, 2nd ed. (Cambridge University Press, New York, USA, 1965).
[23] M. Sigalas, D. A. Papaconstantopoulos, and N. C. Bacalis, Phys. Rev. B **45**, 5777 (1992).
[24] B.-Y. Tsui and C.-F. Huang, IEEE Electron Device Lett. **24**, 153 (2003).
[25] C. Kittel, *Introduction to Solid State Physics*, 7th ed. (Wiley, New York, NY, 1996).
[26] L. Pauling, *The Nature of the Chemical Bond and the Structure of Molecules and Crystals* (Cornell University Press, Ithaca, New York, 1960).
[27] W. Monch, *Semiconductor Surfaces and Interfaces*, 2nd ed. (Springer, New York, 1995).
[28] J. Bardeen, Phys. Rev. **71**, 717 (1947).
[29] D. G. Kelley, M. J. Swartzfager, and V. S. Sundaram, J. Vac. Sci. Technol. **16**, 664 (1979).
[30] S. C. Fain and J. M. McDavid, Phys. Rev. B **9**, 5099 (1974).
[31] D. R. Penn, Phys. Rev. B **35**, 482 (1987).
[32] J. M. Walls and R. Smith, *Surface Science Techniques* (Elsevier Science, Oxford, England, 1994).
[33] M. Ropo, K. Kokko, L. Vitos, J. Kollár, and B. Johansson, Surf. Sci. **600**, 904 (2006).
[34] R. Bouwman, G. J. M. Lippits, and W. M. H. Sachtler, J. Catal. **25**, 350 (1972).
[35] W. M. H. Sachtler and G. J. H. Dorgelo, J. Catal. **4**, 654 (1965).
[36] Y. Takasu, H. Konno, and T. Yamashina, Surf. Sci. **45**, 321 (1974).
[37] K. Y. Yu, C. R. Helms, W. E. Spicer, and P. W. Chye, Phys. Rev. B **15**, 1629 (1977).
[38] R. Ishii, K. Matsumura, A. Sakai, and T. Sakata, Appl. Surf. Sci. **169-170**, 658 (2001).
[39] Y. S. Ng, T. T. Tsong, and S. B. McLane, Phys. Rev. Lett. **42**, 588 (1979).
[40] H. Y. Wang, R. Najafabadi, D. J. Srolovitz, and R. LeSar, Interface Sci. **1**, 7 (1993).
[41] W. M. H. Sachtler and R. Jongepier, J. Catal. **4**, 665 (1965).
[42] P. van der Plank and W. M. H. Sachtler, J. Catal. **12**, 35 (1968).
[43] R. Bouwman and W. M. H. Sachtler, J. Catal. **19**, 127 (1970).
[44] W. Li and D. Y. Li, J. Chem. Phys. **122**, 064708 (2005).